

# **Effect of SMAT Parameters on Microstructural Features using DOE Technique**

M. Chemkhi<sup>1,\*</sup>, D. Retraint<sup>1</sup>, G. Montay<sup>1</sup>, C. Garnier<sup>1</sup>, F. Belahcene<sup>2</sup>

<sup>1</sup> Institut Charles Delaunay, UMR CNRS 6279, LASMIS, STMR, University of Technology of Troyes, 10010 TROYES, FRANCE

\*mahdi.chemkhi@utt.fr, delphine.retraint@utt.fr, guillaume.montay@utt.fr, claude.garnier@utt.fr

<sup>2</sup> ULTRA RS. Technopole de l'Aube en Champagne, 2 rue Gustave Eiffel, 10430 Rosières près Troyes, FRANCE

f.belahcene@ultrars.com

## **Abstract**

SMAT (Surface Mechanical Attrition Treatment) is a beneficial method to improve the fatigue properties of components and structures. This treatment generates surface nanocrystallization as well as strain hardening provided by severe plastic deformation via multidirectional and random shot impacts. Residual stresses, surface roughness, nanocrystalline layer and work hardening are the main surface effects induced by SMAT. They are closely dependant on the choice of the SMAT parameters.

In this paper Design Of Experiment (DOE) technique was used to examine the effect of process parameters such as sonotrode amplitude and processing time on microstructural features of 316L ASTM F138 alloy. The sonotrode amplitude was revealed to be the most influencing SMAT parameter while interaction between factors could not be neglected. Mathematical models linking the process parameters to the surface properties were developed. The choice of the influencing parameters could thus be optimized according to the roughness and/or the micro-hardness evolution.

**Keywords:** SMAT, nanocrystallization, DOE, roughness, micro-hardness, residual stress

## **Introduction**

During the last two decades, great efforts and significant progress have contributed to the development of nanocrystalline surface layer on order to improve materials properties [1, 2]. Recently, a new family of Severe Plastic Deformation (SPD) processes have been developed to generate nanocrystalline surface layer, for example UltraSonic Shot Peening (USSP) [3], Surface Nanocrystallization and Hardening (SNH) [4], Equal Channel Angular Pressing (ECAP) [5] or Surface Mechanical Attrition Treatment (SMAT) [6].

In this work, SMAT parameters were studied. SMAT is a relatively new process derived from conventional shot peening (SP) to generate a nanocrystallised layer on the surface of metallic materials [6]. Both of these processes are based on repeated impacts on the sample surface in order to induce compressive residual stresses. These two techniques present various differences such as the shape, the size and the velocity of the shot [7]. Many differences can be noticed in the effects after SP and SMAT. Compared to SP, SMAT displays an increase in the thickness of the work-hardened layer. Besides, it generates deeper compressive residual stresses beneath the treated surface, with the creation of a superficial nanocrystalline layer. This latter is mainly due to the multidirectional plastic deformation generated by the randomly impacting shot put into motion by a vibrating sonotrode at 20 KHz [6].

Several authors used one-factor-at-a-time approach in analyzing mechanical properties as a function of one SMAT parameter. The shot size effect was thus studied on the fatigue life behaviour [8], on the surface roughness, on the wettability [9] and on the hardness [10]. Moreover, the effect of processing time on the grain size [11] and on the wear resistance [12] was also analyzed. Unfortunately, most of these studies were carried out without taking into account the interactions between these factors and their overall effects. The main objective of this work is thus to use Design Of Experiment (DOE) to examine the effect and interactions of SMAT parameters on micro-hardness and roughness of a stainless steel.

## Experimental procedures

### Material and surface treatments

The studied material was a 316 ASTM F138 austenitic stainless steel coupon (90 mm diameter and 5 mm thickness). The SMAT of the as-received samples was performed using the device described in Fig.1.

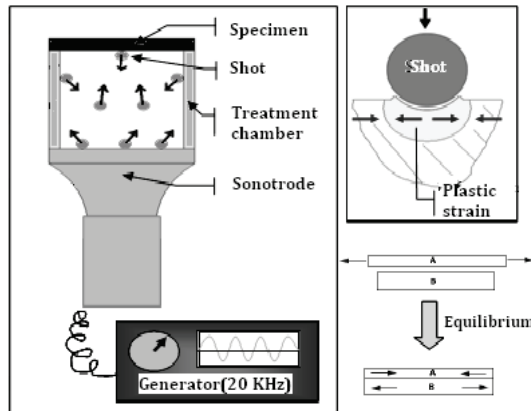


**Figure 1.** Schematic illustration of the SMAT.

As shown in Fig.1, SMAT is based on the vibration of spherical shot (3 mm diameter) thanks to a high frequency (20 KHz) ultrasonic generator. Random shot impacts are generated at the surface of the part to be treated leading to the formation of multidirectional plastic deformation as well as a superficial nanocrystallized layer.

### Material characterization

Surface microhardness measurements were performed in order to evaluate the effect of the processing parameters on the surface layers by using a Vickers microhardness tester. Surface profiles were measured on SMATed and as-received samples by a mechanical contact profilometer 'Surtronic 3+'.

The residual stress field was evaluated by the hole drilling method combined with the digital speckle pattern interferometry. In addition, X-ray diffraction (XRD) measurements were performed to evaluate the superficial residual stress ( $\approx 5\mu\text{m}$  below the surface).

### Design Of Experiment (DOE)

The method of experimental design can give the dominant factors, their influence on the mechanical properties and the interaction between these factors.

The choice of the area of experiment and the identification of the suitable process parameters and their levels are based on screening experiments [8-11-12]. These process parameters are listed in Table 1.

**Table.1.** Factor levels for the experiment

| Factors                  | Lower level |      | Higher level<br>+1 |
|--------------------------|-------------|------|--------------------|
|                          | -1          | 0    |                    |
| P: device Power (%)      | 50          | 68,5 | 87                 |
| T: processing Time (min) | 10          | 20   | 30                 |

The design of experiment was based on full factorial design which considers two factors, each at two levels. In order to reduce process and product variability, three additional trials at the centre of the area of experiment were done. The design matrix considering the further tests and the results of response selected in this study are shown in Table 2.

**Table.2.** Full factorial design matrix

| Experiment no. | T  | P  | S  | Roughness Ra(μm) | Roughness Rt(μm) | Micro-hardness (HV0,025) |
|----------------|----|----|----|------------------|------------------|--------------------------|
| 1              | -1 | -1 | -1 | 0,891            | 4,90             | 527,28                   |
| 2              | +1 | -1 | -1 | 0,788            | 4,55             | 540,2                    |
| 3              | -1 | +1 | -1 | 1,279            | 7,51             | 571,65                   |
| 4              | +1 | +1 | -1 | 1,119            | 6,962            | 626,12                   |
| 5              | 0  | 0  | 0  | 0,944            | 5,02             | 560,04                   |
| 6              | 0  | 0  | 0  | 0,993            | 5,75             | 560,75                   |
| 7              | 0  | 0  | 0  | 0,916            | 5,34             | 562,05                   |

In the present investigation, MINITAB (statistical software) was used to analyze the effect and the interaction between the factors and to illustrate the results.

## Results and discussion

### Surface roughness

The surface roughness after SMAT is an important parameter. An increase of the roughness can indeed reduce the beneficial effects of superficial compressive residual stress and/or of the nanostructure induced by SMAT [13]. Roughness has also an important role on fatigue properties as rough surface profiles can induce stress concentration effect and thus present sites of crack initiation. This negative effect can be expressed linking the stress concentration factor and the total roughness ( $R_t$ ) [14]. Nevertheless, in some cases increase roughness may have a beneficial effect, for example during the development of multilayer structures by the duplex process SMAT/co-rolling treatment [15].

It is very important to control surface roughness during SMAT to improve the fatigue behaviour or to give a good interface bonding of the co-rolled laminate. The analysis of SMAT effect parameters on roughness during the experimental design is shown in Fig.2. With this first experimental design of Fig2a, we can choose the correct parameters between enhance fatigue behaviour and friction tests (when we have a low peak of roughness) or co-rolling treatment (when we have a high peak of roughness).

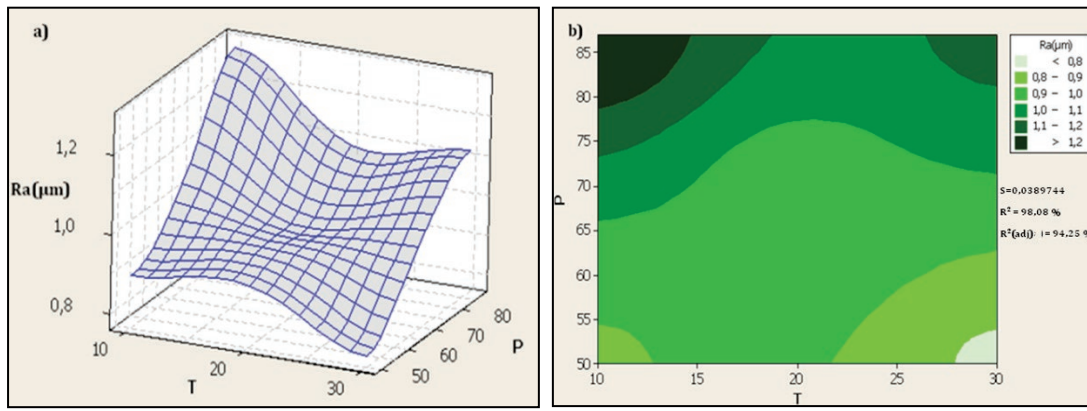


Figure 2. a) Roughness  $R_a$  graphical display b) Contour of  $R_a$  as a function of  $P$  and  $T$ .

Fig2b gives more explanations on the different evolution stages of roughness  $R_a$  as a function of process condition. Thus, the evolution of the measured arithmetic mean value  $R_a$  at the low power level indicates some qualitative similarity for the case of process (SNH) reported in ref [16], namely the surface roughness  $R_a$  increases sharply at the beginning of treatment, and then decreases to achieve a saturation magnitude. However, in high power, the saturation is reached after a shorter time than the low power. It is also important to study the interaction between parameters. The effect of device power (sonotrode amplitude) on roughness  $R_a$  is more predominant than the processing time (Fig3a).

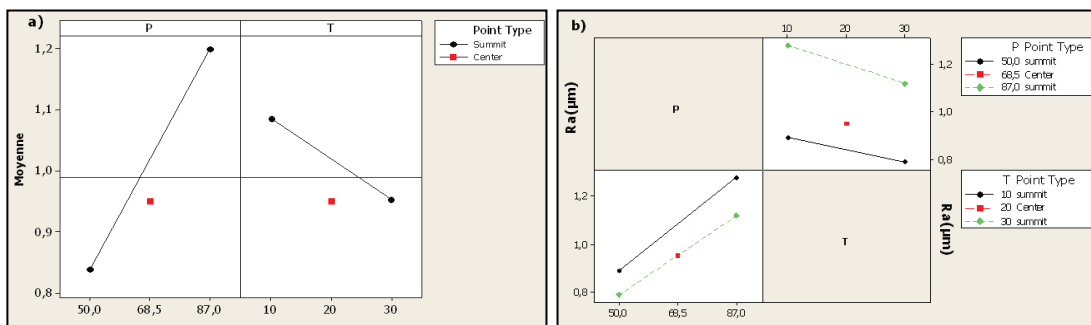


Figure 3. a) Main effects of factors on roughness  $R_a$  b) Interaction effect between factors.

However, it is interesting to note that the line segments in Fig. 3b are parallel, which indicates that the interaction effect between  $P$  and  $T$  on roughness  $R_a$  can be neglected at their lower and higher levels.

Mathematical relationship between the arithmetic mean ( $R_a$ ) and total ( $R_t$ ) roughness and the effects of the studied factors and their interactions were established by developing regression models using Analyze-it software [17].

$$Ra = 0,99 - 0,06575t + 0,17975P - 0,01425tP \quad (R^2 = 98,08 \%) \quad (1)$$

$$Rt = 5,722 - 0,226625t + 1,253875P - 0,049625tP \quad (R^2 = 96,39 \%) \quad (2)$$

The resulting regression equations (1) and (2) yield approximate values of both roughnesses. However, they would serve as a useful guide for selecting proper values of SMAT parameters for the above materials so as to obtain desired property of the component.

#### Residual stress

Like shot-peening, SMAT generates an in-depth residual stress gradient, resulting from the incompatibility of the plastic strain after treatment.

In-depth residual stresses were measured using a combined system of blind-hole drilling and digital speckle pattern interferometry [18]. It is based on the principle of interference between two laser beams and can record not only intensity but also the phase variation of the images. The resulting images, obtained by phase shifting, made it possible to get for each increment the displacement field of the entire surface of the specimen. The sample with test n°1 was taken for illustration (Fig. 4).

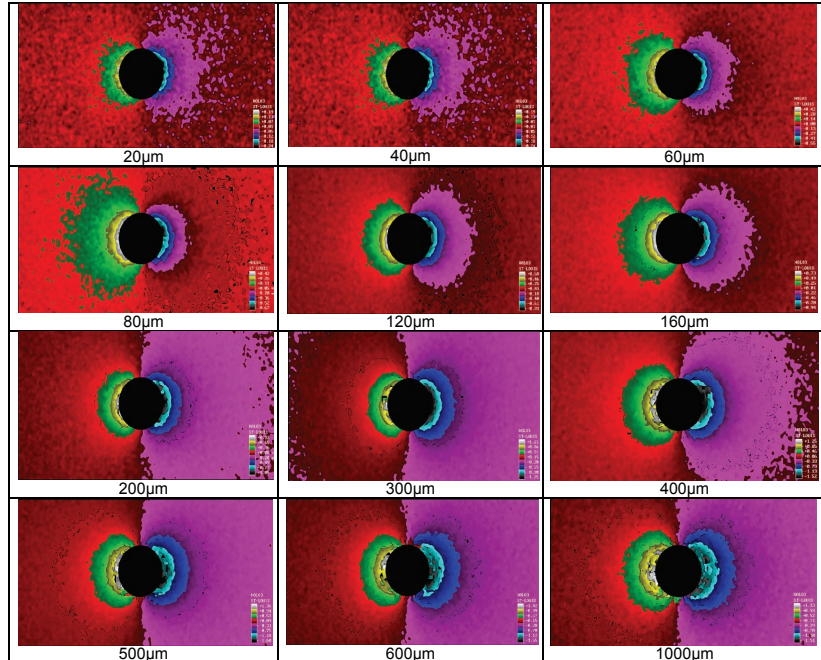


Figure 4. Displacement fringes evolution as a function of hole depth.

The interference fringes are created when the image corresponding to the final state of the object (distorted) is subtracted from the one of the same object in an initial state (undeformed).

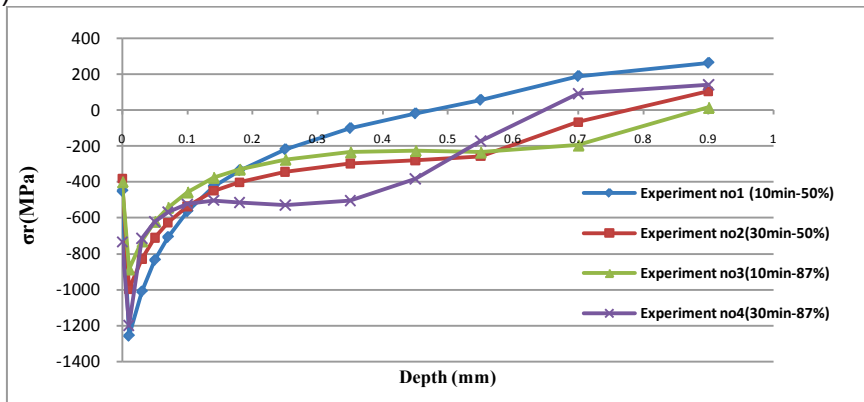


Figure 5. Residual stresses variation with depth.

Figure 5 compares the residual stress profiles generated by different SMAT parameters. The experimental results calculated from X-ray diffraction in the surface and the hole drilling and digital speckle pattern interferometry show that SMAT can generate large compressive

residual stress down to -1000MPa on the austenitic stainless steel surface. Besides, the stress level varies greatly with the SMAT parameters. However this evolution is not clear at the moment. Additional X-ray diffraction measurements at different depths below the surface are in progress.

### Micro-hardness

Surface microhardness measurements were performed on the cross-section of SMATed specimens to investigate the main effect of process parameters and the interaction between them. Typical hardness profiles are shown in Fig.6a. The initial surface hardness is equal to 260 HV<sub>0.025</sub> (test load 25gf), and it increases up to ≈600 HV<sub>0.025</sub> after SMAT. The hardness of the untreated material can thus be increased by a factor of 2-2.5 after SMAT.

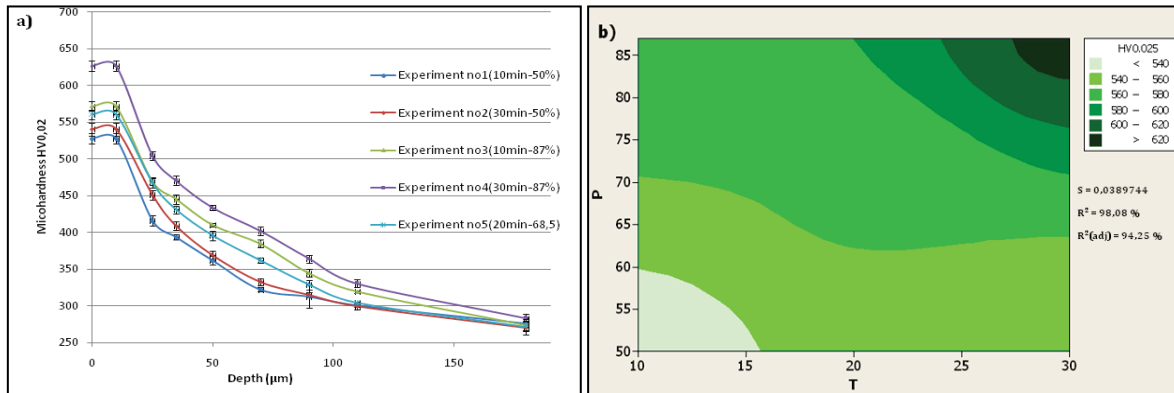


Figure 6.a) Hardness profiles of different treated sample, b) graphical contour plot of HV0.025.

It can be seen in Fig.6b that the effect of two factors studied: the higher the device power or the treatment time is, the higher the micro-hardness becomes.

Figure 7 shows the effects of main factors and interaction effects on the surface hardness.

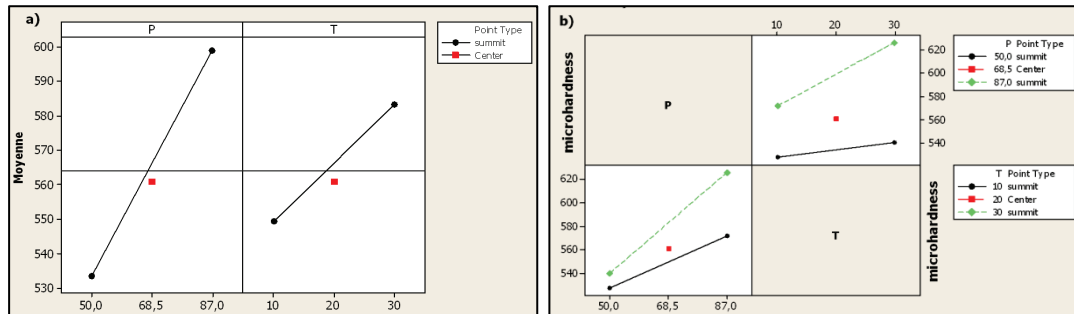


Figure 7. a) Main effects of factors on microhardness b) Interaction effect between factors.

We can conclude that the effect of device power (sonotrode amplitude) on microhardness is greater than the processing time. An interaction effect between P and T on hardness can be noticed in Fig.7b, as the line segments are not parallel.

A relationship between the process parameters and the surface microhardness can be established as follows:

$$HV0,025 = 566,31 + 16,84t + 32,57P + 10,38tP \quad (R^2 = 99,96 \% ) \quad (3)$$

Eq. (3) can be useful for selecting proper values of SMAT parameters to obtain desired values of hardness. Also R<sup>2</sup> ≈ 1 show the relevance of the explanatory variables used in predicting the response.

### Conclusion

This study shows that SMAT can strongly modify the surface features of 316L ASTM F138. The effect of SMAT parameters, device power (P), processing time (T) and their interaction on surface parameters were studied using DOE technique. It was found that the device power is the most important parameter on all the properties studied.

The main effect and the interaction between SMAT parameters were determined using the DOE experimental results. Different mathematical models were established to serve as a

useful guide for setting proper values of process parameters according to the desired surface features of the treated component.

### Acknowledgements

The authors wish to thank the Regional Council of Champagne-Ardenne (France) and Europe (FEDER) for financial support (NANOSURF project).

### References

- [1] H. Gleiter, Nanocrystalline materials, *Prog. Mater. Sci.*, Vol. 33 (1989), pp 223-315.
- [2] Y. Lin et al, Surface nanocrystallization by surface mechanical attrition treatment and its effect on structure and properties of plasma nitrided AISI 321 stainless steel, *Acta Materialia*, Vol.54 (2006), pp 5599–5605.
- [3] X. Wu, N. Tao, Y. Hong, B. Xu, J. Lu, K. Lu, Microstructure and evolution of mechanically-induced ultrafine grain in surface layer of AL-alloy subjected to USSP, *Acta Materialia*, Vol.50 (2002), pp 2075–2084.
- [4] K. Dai, J. Villegas, Z. Stone, L. Shaw, Finite element modeling of the surface roughness of 5052 Al alloy subjected to a surface SPD process, *Acta Materialia*, Vol.52 (2004), pp 5771–5782.
- [5] Y. Iwahashi, Z. Horta, M. Nemoto and Terence G. Langdon, The Process of Grain Refinement in ECAP, *Acta mater.*, Vol. 46, No. 9 (1998), pp. 3317±3331
- [6] K. Lu, J. Lu, Nanostructured surface layer on metallic materials induced by surface mechanical attrition treatment, *Materials Science and Engineering A* 375–377 (2004) 38–45.
- [7] D. Retraint, C. Pilé, C. Garnier, J. Lu, "Ultrasonic shot peening", *Handbook on Residual Stress*, 2nd Edition, Ed. Society for Experimental Mechanics, Vol.1 (2005), pp 146-159 .
- [8] T. Roland D. Retraint, K. Lu, J. Lu, Fatigue life improvement through surface nanostructuring of stainless steel by means of SMAT, *Scripta Mater.* Vol.54 (2006), pp 1949–1954.
- [9] B. Arifvianto, Suyitno, Instrumentation, Communications, Information Technology, and Biomedical Engineering (ICICI-BME), (2009), pp 1-4
- [10] L. Waltz, D. Retraint, A. Roos, P. Olier & J. Lu, Comportement mécanique d'une structure multicouche obtenue par colaminage de tôles nanostructurées par SMAT, 18ème Congrès Français de Mécanique, Grenoble, (2007).
- [11] X. YONG, Characterization and Properties of Nanostructured Surface Layer in a Low Carbon Steel Subjected to SMA, *J. Mater. Sci. Technol.*, Vol.19 No.1 (2003)
- [12] W. Yan , Effect of surface nanocrystallization on abrasive wear properties in Hadfield steel, *Tribology International* 42 (2009), pp 634–641
- [13] S. Bagherifard, Fernández Pariente, R. Ghelichi, M. Guagliano, Fatigue properties of nanocrystallized surfaces obtained by high energy shot peening, *Procedia Engineering* 2 (2010), pp 1683–1690.
- [14] J.K. Li, Mei Yao, Duo Wang and Renzhi Wang, An analysis of stress concentration caused by shot peening and its application in predicting fatigue strength, *Fatigue Fracture Engng Mater. Struct.* 15 (12) (1992), pp 1271–1279.
- [15] L. Waltz, D. Retraint, A. Roos and P. Olier, Combination of surface nanocrystallization and co-rolling: Creating multilayer nanocrystalline composites, *Scripta Materialia*, Vol.60 (2009), pp 21–24.
- [16] K. Dai et al, Finite element modeling of the surface roughness of 5052 Al alloy subjected to a surface severe plastic deformation process, *Acta Materialia*, Vol.52 (2004), pp 5771–5782.
- [17] G.Sado et M-C.Sado, Les plans d'expériences, « De l'expérimentation à l'assurance qualité », AFNOR-Tour Europe-92049 Paris La Défence cedex,(2000)
- [18] F. V. Díaz, G. H. Kaufmann, et al., "Determination of residual stresses using hole drilling and digital speckle pattern interferometry with automated data analysis" *Optics and Lasers in Engineering*, Vol.33 (2000), pp 39-48.